Analysis of Hard Turning Process of AISI D3-Thermal Aspects

B. Varaprasad, C. Srinivasa Rao

Abstract—In the manufacturing sector, hard turning has emerged as vital machining process for cutting hardened steels. Besides many advantages of hard turning operation, one has to implement to achieve close tolerances in terms of surface finish, high product quality, reduced machining time, low operating cost and environmentally friendly characteristics. In the present study, three-dimensional CAE (Computer Aided Engineering) based simulation of hard turning by using commercial software DEFORM 3D has been compared to experimental results of stresses, temperatures and tool forces in machining of AISI D3 steel using mixed Ceramic inserts (CC6050). In the present analysis, orthogonal cutting models are proposed, considering several processing parameters such as cutting speed, feed, and depth of cut. An exhaustive friction modeling at the tool-work interfaces is carried out. Work material flow around the cutting edge is carefully modeled with adaptive re-meshing simulation capability. In process simulations, feed rate and cutting speed are constant (i.e.,. 0.075 mm/rev and 155 m/min), and analysis is focused on stresses, forces, and temperatures during machining. Close agreement is observed between CAE simulation and experimental values.

Keywords—Hard-turning, computer-aided engineering, computational machining, finite element method.

I. INTRODUCTION

MACHINING is quite popular manufacturing process in the manufacturing sector of high precision distinct metal parts. With advent of new kind of tools such as Cubic Boron Nitride (CBN), Polycrystalline Cubic Boron Nitride (PCBN), polycrystalline diamond (PCD), coated, Chemical Vapor Deposition (CVD), Physical Vapor Deposition (PVD) and ceramic tools, better surface finish will be accessible without any finishing and complementary operation such as grinding. Turning of hardened steels into finished parts by eliminating intermediate machining and reducing grinding processes has been a cost effective method for manufacturing high-quality automotive components [1].

Besides, hard turning is flexible, environmentally-friendly and higher output substitute to cylindrical grinding. However, surface quality and process reliability are still considered not on par with grinding processes, due to issues related to different geometrically defined cutting tools [2].

The manufacturing sector is still hesitating to implement

B. Varaprasad is an Assistant Professor in Mechanical Engineering Department, GVP College for Degree and PG studies, School of Engineering, Technical Campus, Rushi-Konda, Visakhapatnam, India (phone: 08912790084, fax: 08912737719, e-mail: varaprasad.bhimuni11 @gmail.com).

C. Srinivasa Rao is a Professor in the Department of Mechanical Engineering, College of Engineering, Andhra University, Visakhapatnam, India (e-mail: csr_auce@yahoo.co.in).

fast and economic hard turning technology compared to slow and costly grinding. Ceramic cutting tools can withstand high temperatures but not thermal and mechanical shocks. To optimize the tooling cost, ceramic cutting tools are right candidates for light and continuous cutting. The geometry of the insert also has a major influence on the surface integrity; single point cutting tool gives uniform microstructural changes compared to grinding as this will increase the functional performance of the product. Hence correct tool geometry must be selected for a given application or may produce subsurface damage and high tensile residual stresses on the surface of the machined workpiece [2]-[5]. Generation of heat during hard turning and heat dissipation along the insert corner is also affected by geometry due to change in work material flow around the cutting edge [3].

Al2O3/TiN-coated tungsten carbide tools for finish-turning of NiCr20TiAl nickel-based alloy under various cutting conditions, cutting forces, surface integrity, and tool wear are investigated, and the inter-diffusing and transferring of elements between Al2O3/TiN-coated tungsten carbide tool and NiCr20TiAl nickel-based alloy are studied [6]. The cutting performance of tungsten carbide tools with restricted contact length and multilayer chemical vapor deposition coatings, TiCN/Al2O3/TiN and TiCN/Al2O3–TiN in the dry turning of AISI 4140 and the results show that coating layouts and cutting tool edge geometry can significantly affect heat distribution into the cutting tool [7].

The machinability of hardened steel using gray relational approach and ANOVA to obtain optimum process parameters considering MRR, surface finish, tool wear and tool life for both rough and finish machining [8]. Multi-response optimization of turning parameters and nose radius over surface roughness and power consumed using Taguchi based gray relational approach and found that the main influencing parameter is cutting speed followed by feed rate and depth of cut [9].

Mechanics and dynamics of machining hard metals using mixed ceramic tool have been investigated experimentally and analytically in few studies. In addition, studies of Finite Element (FE) modeling, orthogonal two-dimensional cutting are also used to determine the influence of process parameters on performance characteristic such as the formation of the chip, cutting forces, temperatures and effective stresses [10]-[14]. Serrated formation of the chip is also exposed with growing cutting speed and rate of feed in most FE experimental studies in hard turning [14], [15]. On the other hand, FE analyses on three-dimensional hard turning are insufficient to appreciate process completely. Established a

three-dimensional FE model for turning to predict forces of cutting, temperature and distribution of stresses for the machining of aluminum alloys and low-carbon steels under orthogonal and oblique cutting configurations [16]. Acclaimed a three-dimensional FE model for the hard turning of AISI 52100 steel using PCBN tools [17]. Aurich et al. offered three-dimensional FE modeling for segmented chip formation [18].

It is found from the literature that there is a scope for comparing CAE analysis with experimental results. The main advantage of CAE analysis over experimentation is that simulation can be performed for a wide range of input parameters to enumerate their behavior on performance characteristics. Rosochowska et al. [19] experimentally compared the heat contact conductance h with theoretical formulation at various contact pressures and different temperatures. Therefore, a heat transfer coefficient h is found using the formulation from the Nusselt number as provided in Incropera and Dewitt [20].

II. EXPERIMENTATION

The workpiece material used for experimentation is AISI D3. Bars of diameter 70 mm x 360 mm long are prepared. The test sample is true-centered and cleaned by removing a 2 mm layer prior to actual machining tests. The chemical composition of the workpiece materials are given in Table I. The AISI D3 is oil-quenched from 980oC for hardening, followed by tempering at 200oC to attain 62HRC. The experimental setup is shown in Fig. 1.
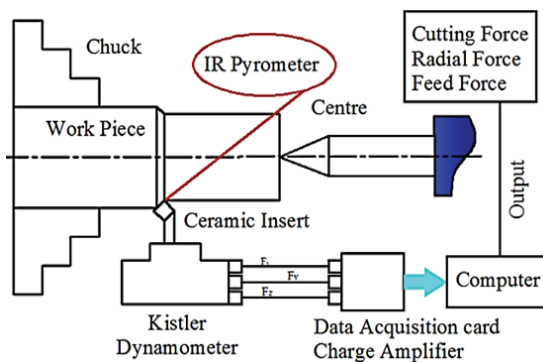

Fig. 1 Experimental setup

The lathe used for machining operations is Kirloskar; model Turn Master-35, spindle power 6.6KW. The cutting forces are measured by Kistler piezoelectric dynamometer (model 9257B). This dynamometer can measure forces in three mutually perpendicular directions i.e. F_x (Feed Force), F_y (Thrust Force (0 to 5000N)) and F_z (Cutting Force (0 to 10000N)). The charge generated at the dynamometer is amplified by a Kistler charge amplifier (model 5070A). The signal is acquired by a data acquisition system consists of a personal computer as controller and cable for PC to charge amplifier connection. The Dynoware software installed in the PC is used to see the continuous flow of data for force in all three directions. The average value of this force data was used for further analysis.

Surface roughness is measured using Mitutoyo Surftest SJ 210 having a measuring range of 17.5mm and skid force less than 400 mN. Four readings with a sample length of 0.8 mm are recorded after each experiment, and an average value is taken as the surface roughness.

TABLE I
CHEMICAL COMPOSITION OF AISI D3 (WT %)

Constitution	%
C	2.06
Si	0.55
Mn	0.449
P	0.036
S	0.056
Cr	11.09
Ni	0.277
Mo	0.207
Al	0.0034
Cu	0.13
Zn	0.27
Fe	Balance

The Ra values are obtained without disturbing the assembly of the workpiece in order to reduce uncertainties. The cutting insert used is having designation SNGA 120408 T01020 a mixed ceramic grade (Make: Sandvik CC6050) based on alumina with an addition of titanium carbide. The high hot hardness, the good level of toughness makes the grade suitable as the first choice for machining hardened steels (50 – 65HRC) in applications with good stability or with light interrupted cuts. The inserts are mounted on a commercial tool holder of designation PSBNR 2525 M 12 (ISO) with the geometry of active part characterized by the following angles $\chi = 75°$; $\alpha = 6°$; $\gamma = -6°$; $\neg\lambda = -6°$.

The temperature of the machined samples are measured by the use of infrared thermometer (Make: Amprobe IR750) having a temperature range of -50°C to 1500°C and with an optical resolution of 10:1 and emissivity 0.1 - 1 (adjustable). Three levels are defined for each cutting process parameters as given in Table II. The cutting process parameters levels are chosen within the intervals according to recommendations made by the cutting tool manufacturer. Three selected cutting process parameters at three levels led to a total of 20 tests as per the Response Surface Methodology (RSM) based Central Composite Design (CCD) is applied as an experimental design employed to accomplish 20 tests with six center points. The six axial runs have the same input parameters; therefore, the design matrix has six repeated runs.

TABLE II
ASSIGNMENT OF THE LEVELS TO THE PARAMETERS

Parameters	Range		
	-1	0	+1
Speed(m/min)	145	155	165
Feed(mm/rev)	0.05	0.075	0.1
Depth of cut(mm)	0.3	0.6	0.9

III. COMPUTATIONAL MODELLING OF 3D TURNING

In present work the CAE software DEFORM 3D is based on an implicit Lagrangian computational routine with continuous adaptive re-meshing. The workpiece is modeled as perfectly plastic material where the constitutive material model of this deformable body is represented with Johnson–Cook material model [21] (as in (1)) where $\bar{\sigma}$ is flow stress, ε is the plastic strain, $\dot{\varepsilon}$ is the plastic strain rate, $\dot{\varepsilon}_0$ is the reference plastic strain rate (0.001s-1), T is the temperature of the workpiece, T_{melt} is the melting temperature of the workpiece material and T_o is the room temperature. Material constant A is the yield strength, B is the hardening modulus, C is the strain rate sensitivity, n is the strain-hardening exponent and m the thermal softening exponent. Although a more realistic simulation model for the machining process should also take A=1491MPa, B = 570MPa, n = 0.24, C = 0.0027, m= 0.6, T_{melt} = 1450 $^{o\,C}$ for AISI D3.

$$\bar{\sigma} = [A + B(\varepsilon)^n]\left[1 + C\ln\left(\frac{\dot{\varepsilon}}{\dot{\varepsilon}_0}\right)\right]\left[1 - \left(\frac{T-T_o}{T_{melt}-T_o}\right)^m\right] \qquad (1)$$

The workpiece is represented by a straight model of 10mm where the cutting tool is modeled as a rigid body which moves at the specified cutting speed. A fine mesh density is defined as an input size of 0.075mm and size ratio 2 for the workpiece. Thermal boundary conditions are defined in view of that it will allow heat transfer from the workpiece to cutting tool. Heat transfer between the workpiece and tool is dependent on the pressure developed during machining. Thermal and Mechanical properties used in the present paper are taken from the literature sources those values are mentioned in Table III. Workpiece model includes 100000 elements of tetrahedron shape. The bottom surface of the workpiece is fixed in all directions. The cutting tool is modeled as a rigid body using 25000 (Shape: Tetra hydron) elements which move at the specified cutting speed. A fine mesh density is defined at the tip of the tool and at the cutting zone to obtain fine process output distributions. 3D computational modeling is utilized to predict chip formation, forces, temperatures, and tool wear on the uniform honed tool of 80-micron nose radius. All simulations are run at the same cutting condition (V = 155 m/min, f=0.075 mm/rev, ap = 0.6 mm) for machining of AISI D3 steel at 62 HRC hardness

TABLE III
THERMO-MECHANICAL PROPERTIES OF WORK AND TOOL MATERIALS

Properties	AISI D3	Ceramics
Density (kg m^{-3})	7700.00	3980.00
Modulus of elasticity (GPa)	0200.00	0300.00
Poisson's ratio	0000.29	0000.21
Specific heat (J kg−1 K−1)	0460.00	0880.00
Thermal conductivity (Wm−1 K−1)	0020.00	0018.00
Thermal expansion (mm−1 K−1)	0012.30	0008.10

IV. RESULTS AND DISCUSSION

As mentioned Section III, the experimental results obtained from the various measuring equipment is shown in Table IV. The obtained data from experimentation is compared with the simulation results from DEFORM 3D software for the materials AISI D3.

TABLE IV
EXPERIMENTAL RESULTS OF CUTTING FORCES, SPECIFIC CUTTING FORCE, POWER, AND SURFACE ROUGHNESS OF AISI D3

Sl. No.	Speed (V_c) (m/min)	Feed (f) (mm/rev)	DOC(a_p) (mm)	Resultant Force F(N)	Specific Cutting Force K_s (N/mm2)	Power P (kW)	R_a(μm)	Temperature (°C)
1	145	0.050	0.3	207.48	7533.3	0.273	1.33	376
2	165	0.050	0.3	250.75	6846.6	0.317	1.88	331
3	145	0.100	0.3	307.06	5000.0	0.362	0.90	341
4	165	0.100	0.3	342.52	6486.6	0.535	0.82	405
5	145	0.050	0.9	526.19	6422.2	0.698	2.06	428
6	165	0.050	0.9	532.66	6935.5	0.858	2.11	418
7	145	0.100	0.9	586.72	3722.2	0.809	1.10	515
8	165	0.100	0.9	522.68	3120.6	0.913	0.91	404
9	145	0.075	0.6	414.05	4888.8	0.531	0.84	376
10	165	0.075	0.6	443.62	5451.1	0.674	0.93	349
11	155	0.050	0.6	397.21	7213.3	0.559	2.27	335
12	155	0.100	0.6	514.47	5175.0	0.802	0.93	365
13	155	0.075	0.3	235.64	5555.5	0.322	1.05	352
14	155	0.075	0.9	482.74	3899.4	0.679	0.83	431
15	155	0.075	0.6	444.47	5604.4	0.651	0.71	353
16	155	0.075	0.6	444.86	5777.7	0.671	0.76	364
17	155	0.075	0.6	453.99	5733.3	0.666	0.73	345
18	155	0.075	0.6	449.76	5511.1	0.640	0.75	371
19	155	0.075	0.6	459.40	5822.2	0.676	0.74	339
20	155	0.075	0.6	460.59	5666.6	0.658	0.72	381

A. Influence of Uniform Honed Insert on Temperature Fields

The insert (CC6050) is used for the present research due to its utilization in the local metal cutting industry for its high material removal rate and realization of good surface finish for the experimentation. Friction in metal cutting is found complex due to the varying level of contact conditions along the tool–chip contact area. In 3D FE modeling, constant shear friction factor, m, Coulomb friction, μ, and pressure-dependent shear friction factor, m (p), have been benchmarked to identify the friction between tool and workpiece. The pressure dependent friction factor for the conditions (V=155 m/min, f=0.075 mm/rev, ap=0.6 mm) is evaluated from experimentation and is used in the modeling. A simple trial-and-error approach is used during fine-tuning friction models for calibrating FE simulation outputs.
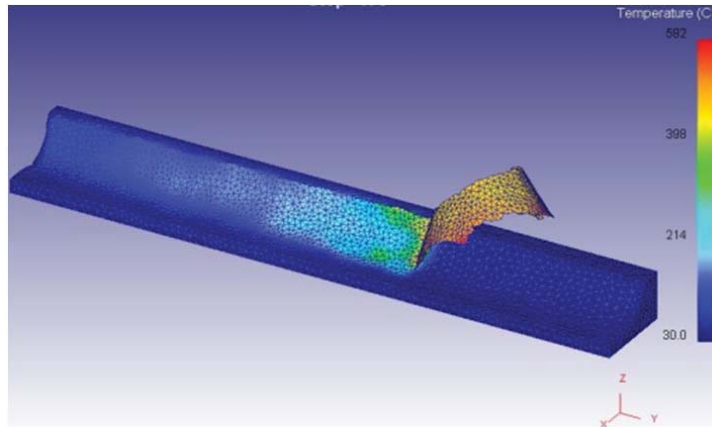

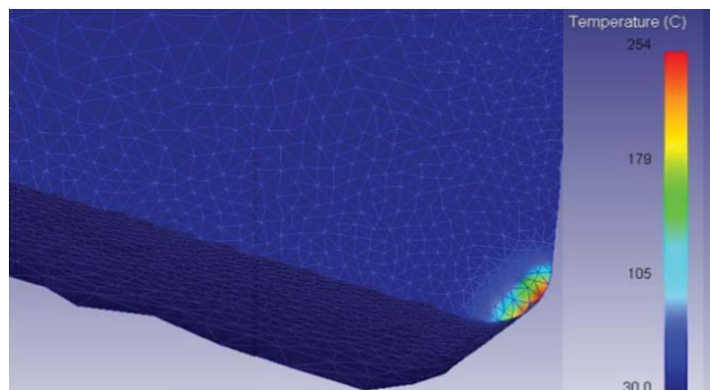Fig. 2 Workpiece Temperature Profile of AISI D3

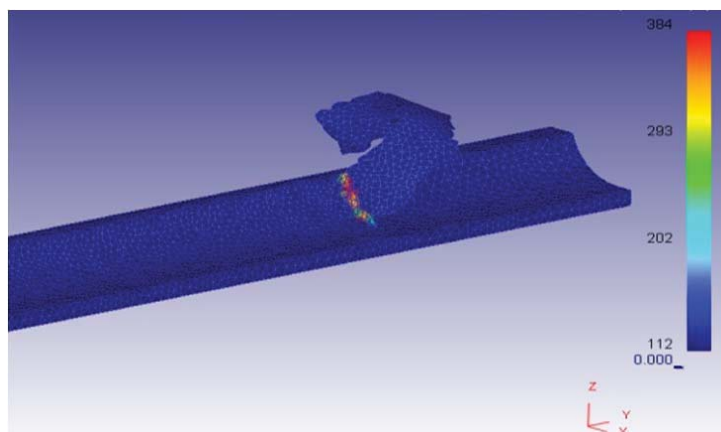Fig. 3 Tool Temperature Profile While Cutting AISI D3

Fig. 4 Interface Temperature Profile While Cutting AISI D3

After careful considerations in all aspects, the form of the results is similar for all conditions, except the magnitude. From the results obtained, it may be concluded that the maximum temperature workpiece and tool increases with increasing cutting speed, being 353°C from Table V when machining AISI D3 at constant cutting speed (155 m/min) considered. Fig. 2 shows simulated values obtained during the machining of AISI D3 workpiece is 582°C. Therefore it is possible, besides the cutting and thrust forces, to extract from the proposed model predictions for values that it would be very laborious or even impossible to obtain otherwise.

As it can be observed from the simulations of the tool, temperatures are 254°C when machining AISI D3 presented in Fig. 3. Examples of such cases are the temperature distribution in the workpiece and tool in the form of isothermal bands and the effective stresses developed during cutting. This explains that the thrust force decreases for higher cutting speed, since softening of the material for higher temperature takes place. The regions that are mostly thermally loaded are the chip and the rake face of the tool, in the chip-tool interface close to tool tip, due to the plastic deformation of the chip and the frictional forces; the part of the chip that is curled away from the rake face is progressively cooled down. The stress has an almost constant value along the center of the shear zone, while near the tool tip, lower values of stress is observed, this can be explained due to the temperature rise of this area which softens the material.

Fig. 4 shows the details of work piece-tool interface temperature. Simulated results for temperature are presented: the values are in the range of 30-592°C when machining AISI D3 and experimental results found to be in the above, said range. With the numerical results provided by the model, it is possible to minimize unwanted effects and to choose suitable cutting conditions in order to optimize the process.
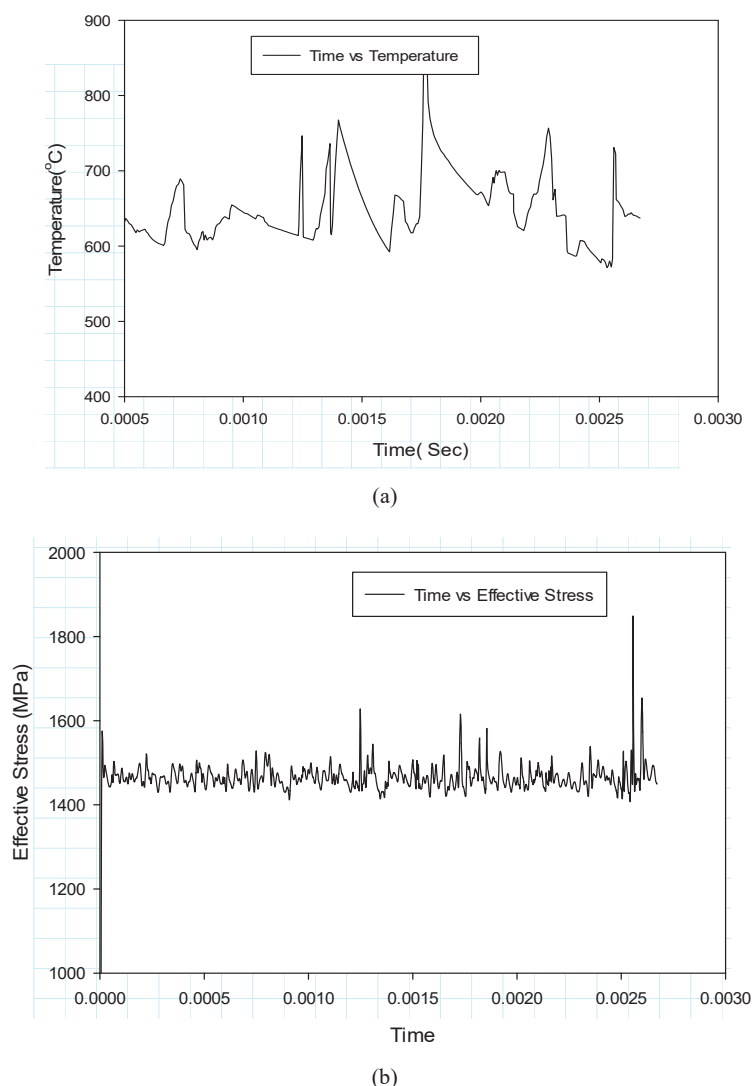

(a)

(b)

Fig. 5 (a) Temperature vs Time while cutting AISI D3 (b) Stress distribution curve AISI D3

The values of temperatures obtained experimentally are found (Table IV) to be correlating with the values from DEFORM 3D simulation. Fig. 5 (a) shows the variations in temperatures with respect to time. The stresses calculated by considering resultant forces are taken into considerations and the results obtained by simulations are correlated. Effective stress profiles are presented in Fig. 5 (b), and they show that the experimental values coincide with simulated results.

V. Conclusions

In the present, experimental and FE modeling investigations on 3D turning with mixed ceramic inserts are presented. Cutting experiments and 3D finite element simulations are performed uniformly honed tool. 3D FE modeling is utilized to predict chip formation, forces, temperatures, stresses and tool wear.

1. The surface roughness of 0.71 for AISI D3 material is obtained at cutting velocity of 155 (m/min), the feed rate of 0.075 (mm/rev) and depth of cut 0.6 mm from the experimental results while machining.

2. The heat generation and stress concentration along the tool cutting edge are more significant, and this can affect tool life, therefore, some limitations to do extensive experimentation with respect to the economy. In the case of CAE, large data generated that can be utilized to predict performance characteristics.

3. Good agreement has shown in the case of tool temperature in both the experimentation and CAE, simulated results for both AISI D3 material.

4. The outcome may be seen as favorable for many performance characteristics, and further investigations may be required on factors which damage the machined surfaces.

References

[1] Byrne, G., Dornfeld, D., Denkena, B., 2003. Advanced cutting technology. Annals of the CIRP 52 (2), 483–507.

[2] Klocke, F., Brinksmeier, E., Weinert, K., 2005. Capability profile of hard cutting and grinding processes. Annals of the CIRP 54 (2), 557–580.

[3] Klocke, F., Kratz, H., 2005. Advanced tool edge geometry for high precision hard turning. Annals of the CIRP 54 (1), 47–50.

[4] Denkena, B., Becker, J.C., de Leon-Garcia, L., 2005. Study of the influence of the cutting edge microgeometry on the cutting forces and wear behavior in turning operations. In: Proceedings of the 8th CIRP, International Workshop on Modelling of Machining Operations, Chemnitz, Germany, pp. 503–507.

[5] Özel, T., Hsu, T.-K., Zeren, E., 2005. Effects of cutting edge geometry, workpiece hardness, feed rate and cutting speed on surface roughness and forces in finish turning of hardened AISI H13 steel. International Journal of AdvancedManufacturing Technology 25, 262–269.

[6] Zou B., Chen M., and Li S., 2011, "Study on finish-turning of NiCr20TiAl nickel-based alloy using Al2O3/TiNcoated carbide tools". International Journal of Advanced Manufacturing Technology, Vol.53, p.81–92.

[7] Fahad M., Mativenga PT., and Sheikh MA., 2012, "A comparative study of multilayer and functionally graded coated tools in high-speed machining", International Journal of Advanced Manufacturing Technology, Vol. 62, p. 43–57.

[8] Gopalsamy BM., Mondal B., and Ghosh S., 2009, "Optimisation of machining parameters for hard machining: grey relational theory approach and ANOVA". International Journal of Advanced Manufacturing Technology, Vol.45, p.1068-1086.

[9] Ahilan C., Kumanan S., and Sivakumaran N., 2010, "Application of Grey based Taguchi method in multi response optimization of turning process". Advances in Production Engineering & Management, Vol. 5(3), p. 171- 180.

[10] Özel, T., 2003. Modeling of hard part machining: effect of insert edge preparation for CBN cutting tools. Journal of Materials Processing Technology 141, 284– 293.

[11] Yen, Y.C., Jain, A., Altan, T., 2004. A finite element analysis of orthogonal machining using different tool edge geometry. Journal of Materials Processing Technology 146, 72–81.

[12] Hua, J., Shivpuri, R., Cheng, X., Bedekar, V., Matsumoto, Y. Hashimoto, F., Watkins, T.R., 2005. Effect of feed rate,workpiece hardness and cutting edge on subsurface residual stress in hard turning of bearing steel using chamfer and hone edge geometry. Materials Science and Engineering A394, 238–248.

[13] Chen, L., ElWardany, T.I., Nasr, M., Elbestawi, M.A., 2006. Effects of edge preparation and feed when hard turning a hotwork die steel with polycrystalline cubic boron nitride tools. Annals of the CIRP 55 (1), 88–92.

[14] Umbrello, D., Rizzuti, S., Outeiro, J.C., Shivpuri, R., M'Saoubi, R., 2008. Hardnessbased flowstress for numerical simulation of hardmachining AISI H13 tool steel. Journal of Materials Processing Technology 199 (1–3), 64–73.

[15] Karpat, Y., Özel, T., 2008a. Mechanics of high speed machining with curvilinear tools. International Journal of Machine Tools and Manufacture 49, 195–208.

[16] Ceretti, E., Lazzaroni, C., Menegardo, L., Altan, T., 2000. Turning simulations using a three-dimensional FEM code. Journal of Materials Processing Technology 98,99–103.

[17] Guo, Y., Liu, C.R., 2002. 3D FEA modeling of hard turning. ASME Journal of Manufacturing Science and Engineering 124, 189–199.

[18] Aurich, J.C., Bil, H., 2006. 3D finite element modelling of segmented chip formation. Annals of the CIRP 55 (1), 47–50.

[19] Rosochowska, M., Balendra, R., Chodnikiewicz, K., 2003. Measurements of thermal conductance. Journal of Materials Processing Technology 135, 204–210.

[20] Incropera. F.P., and DeWitt, D.P.,2001, Fundamentals of Heat and MassTra, Willey, Newyork.

[21] G.R. Johnson and W.H. Cook, Engineering Fracture Mechanics, 21(1985), 31.